

^{199}Hg and ^{63}Cu NMR in superconducting $\text{HgBa}_2\text{CuO}_{4+\delta}$ oriented powder

B. J. Suh, F. Borsa,* J. Sok,[†] D. R. Torgeson, and Ming Xu

Ames Laboratory and Department of Physics and Astronomy, Iowa State University, Ames, Iowa 50011

Q. Xiong

Department of Physics, High Density Electronics Center, University of Arkansas, Fayetteville, Arkansas 72701

C. W. Chu

Department of Physics and the Texas Center for Superconductivity at the University of Houston, Houston, Texas 77204

(Received 28 August 1995; revised manuscript received 20 February 1996)

^{199}Hg NMR measurements have been performed both in the normal and in the superconducting state for an oriented $\text{HgBa}_2\text{CuO}_{4+\delta}$ superconducting powder sample with $T_c=96$ K. The large anisotropic Knight shift of ^{199}Hg , $^{199}K_{\text{ax}}=-0.15\%$ at room temperature, is explained by the chemical shift related to the linear Hg-O(2) bonding configuration. Both $^{199}K_{\text{iso}}$ and $^{199}K_{\text{ax}}$ decrease below T_c and scale linearly with each other in the whole temperature range investigated. The ^{199}Hg Knight shift ^{199}K slowly decreases with decreasing temperature on approaching T_c in the normal state, reflecting the decrease of the uniform spin susceptibility $\chi'(0,0)$ with lowering temperature. The ^{199}Hg spin-echo decay can be fit by the product of a Gaussian component (T_G^{-1}) and an exponential one (T_L^{-1}). The Gaussian component T_G^{-1} which is dominant above T_c , is shown to be due mainly to an indirect nuclear interaction via the conduction electrons (holes) and is found to be directly proportional to the spin contribution ($^{199}K^{\text{sp}}$) of the Knight shift. The exponential component T_L^{-1} becomes dominant well below T_c and is ascribed to the effect of thermal motion of flux lines. The ^{199}Hg nuclear spin-lattice relaxation rate T_1^{-1} in the normal state shows a Korringa behavior well above T_c with $(T_1T)^{-1}=0.1 \text{ sec}^{-1} \text{ K}^{-1}$. Reduction of $(T_1T)^{-1}$ with decreasing temperature is observed starting about 10 K above T_c and is consistent with the decrease of $\chi'(0,0)$ in the normal state observed in $K(T)$ and T_G^{-1} . $^{199}K^{\text{sp}}(T)$ was extracted using the Korringa relation and below T_c , is found to fit the d -wave pairing scheme with a superconducting gap parameter $2\Delta_0=3.5k_B T_c$. The d -wave pairing is also supported by the temperature dependence of ^{199}Hg T_1^{-1} in the superconducting state. The ^{63}Cu T_1^{-1} and T_2^{-1} measurements have been performed in the normal state. In contrast to the Korringa behavior of ^{199}Hg T_1^{-1} in the normal state, the preliminary results show the increase of the ^{63}Cu $(T_1T)^{-1}$ with decreasing temperature, indicating the enhancement of the antiferromagnetic fluctuations of Cu^{2+} moments common in the high- T_c cuprates. The reduction of ^{63}Cu $(T_1T)^{-1}$ is observed starting above T_c and is compared with the decrease of ^{199}Hg K^{sp} , T_G^{-1} , and $(T_1T)^{-1}$ in the normal state. The ^{63}Cu nuclear spin-spin relaxation T_2^{-1} is found to follow an exponential decay in the normal state and to decrease with decreasing temperature similar to the ^{199}Hg K^{sp} and T_G^{-1} .
[S0163-1829(96)01025-9]

I. INTRODUCTION

NMR (nuclear magnetic resonance), as a microscopic probe of local magnetic fields, has played an important role in investigating electronic properties¹⁻³ and vortex dynamics of high- T_c superconductors (HTSC).⁴

$\text{HgBa}_2\text{CuO}_{4+\delta}$ (Hg1201) which has the highest critical temperature, T_c , among the single CuO_2 layered compounds, is a good system for an NMR study of HTSC because of its relative simple structure⁵ and its stability with respect to oxygen stoichiometry. There is only one kind of Cu site in the usual square-planar coordination with four oxygen atoms in the same plane of the Cu. The copper-oxide planes are linked by O-Hg-O chains which involve the apical oxygens [denoted O(2)]. As proved in the preliminary ^{199}Hg NMR study in Hg1201 powder sample,⁶ ^{199}Hg nucleus ($I=\frac{1}{2}$) is a promising probe for an NMR study of the properties of the Fermi liquid because (i) there is no perturbation due to quadrupole interaction, and (ii) the large atomic hyperfine coupling constant allows one to have a sensitive probe of the behavior of

the Fermi liquid. In addition, the symmetric location of Hg in the crystal lattice can afford a probe to test the existence of the (antiferromagnetic) correlations between adjacent CuO_2 planes.

In this paper, we report a ^{199}Hg and ^{63}Cu NMR study in an oriented sample of single-phase Hg1201 with $T_c=96$ K aimed at the microscopic study of the behavior of the Fermi liquid both in the normal and in the superconducting state. The ^{199}Hg Knight shift (K), the nuclear spin-spin relaxation rate (T_2^{-1}), and the nuclear spin-lattice relaxation rate (NSLR, T_1^{-1}) have been measured as functions of temperature for two crystal orientations with respect to the applied field \mathbf{H} ; $\mathbf{H}\parallel\mathbf{c}$ and $\mathbf{H}\perp\mathbf{c}$. All the ^{199}Hg NMR parameters are found to be driven by the coupling with the Fermi liquid of the charge carriers and they give information about the spin susceptibility in both the normal and the superconducting state including the superconducting energy gap and the symmetry of pairing in the superconducting state. A small anisotropy in the relaxation rate with respect to the magnetic-field orientation is observed below T_c and above the irreversibility

temperature. The effect can be ascribed to a contribution to nuclear relaxation associated with the thermal motion of vortices as discussed in a separate publication.⁷ The ⁶³Cu NSLR has also been measured for **H**_{||c} to investigate the antiferromagnetic fluctuations and the problem of the opening of a spin pseudogap.

The paper is organized as follows. In Sec. II we introduce the NMR background which is helpful to understand this paper. In Sec. III we present the experimental details and in Sec. IV the ¹⁹⁹Hg and ⁶³Cu NMR results. Data analysis and discussion are given in Sec. V followed by summary and conclusions in Sec. VI.

II. NMR BACKGROUND

Nuclear magnetic resonance (NMR) measurements provide local microscopic information about both static equilibrium properties through the line shift and dynamic properties through the nuclear relaxation rates. A time-dependent local magnetic hyperfine field **H**_{loc} is generated by the electron spin or the electron orbital motion. NMR parameters such as K , T_1^{-1} , and T_2^{-1} monitor the hyperfine interaction between the nuclear spins and **H**_{loc}.^{8,9} The shift tensor K expresses the NMR line shift from the Larmor frequency and reflects the time average of **H**_{loc}. The total shift K^{tot} can be decomposed in general into spin (K^{sp}) and orbital contributions (K^{orb})

$$K_{\alpha}^{\text{tot}}(T) = K_{\alpha}^{\text{sp}}(T) + K_{\alpha}^{\text{orb}}, \quad (1)$$

where α is an index which specifies the orientation of the external magnetic field with respect to the crystal axis system and K^{orb} is the sum of the Van Vleck term K^{VV} and the chemical shift δ .

The two contributions to K in Eq. (1) can be expressed in terms of the hyperfine coupling constant A and of the static local susceptibility χ as^{8,9}

$$\begin{aligned} K_{\alpha}^{\text{sp}} &= A_{\alpha}^{\text{sp}} \chi_{\alpha}^{\text{sp}}, \\ K_{\alpha}^{\text{orb}} &= A_{\alpha}^{\text{orb}} \chi_{\alpha}^{\text{orb}} + \delta. \end{aligned} \quad (2)$$

Below the superconducting transition temperature (T_c), K^{orb} remains temperature independent, whereas K^{sp} is expected to decrease with decreasing temperature in the superconducting state due to the decrease of the quasiparticle density of state at the Fermi level as a result of the opening of the superconducting gap.

For an axially symmetric shift tensor, the isotropic (K_{iso}) and the axial component (K_{ax}) are defined as⁹

$$\begin{aligned} K_{\text{iso}} &= \frac{1}{3} (K_{\parallel} + 2K_{\perp}), \\ K_{\text{ax}} &= \frac{1}{3} (K_{\parallel} - K_{\perp}), \end{aligned} \quad (3)$$

where K_{\parallel} (K_{\perp}) denotes the Knight shift for the applied field parallel (perpendicular) to the axially symmetric c axis of the crystal. In measuring the Knight shift below T_c one should take into account the macroscopic contribution due to the magnetization¹⁰

$$K^{\text{meas}}(T) = K(T) + 4\pi(1-N) \frac{M(T)}{H} \quad (\text{in cgs unit}), \quad (4)$$

where K^{meas} is the measured Knight shift and K is the intrinsic one. Both the magnetization M and the external magnetic field H are in Gauss units. The demagnetization factor N for a granular sample is not uniform. An average value $N=0.45$ is often assumed, independently of the orientation of the external magnetic field.¹

The fluctuating part of the local hyperfine magnetic field is the source of the nuclear spin-lattice relaxation. The NSLR T_1^{-1} , can be written quite generally in terms of the generalized dynamical spin susceptibility χ' and of the nuclear-electron hyperfine coupling constants A as¹¹

$$\begin{aligned} \left(\frac{1}{T_1 T} \right)_{\alpha} &= 4 \gamma_N^2 k_B \sum_q |A_{\alpha}(\mathbf{q})|^2 \frac{\chi''(\mathbf{q}, \omega_0)}{\omega_0}, \\ A_{\alpha}(\mathbf{q}) &= \sum_j (A_j)_{\alpha} e^{i\mathbf{q} \cdot \mathbf{r}}, \end{aligned} \quad (5)$$

where ω_0 is the nuclear resonance frequency, γ_N is the nuclear gyromagnetic ratio, and k_B is the Boltzman constant. The presence of the filtering factors $A(q)$ in Eq. (5) allows one to use different nuclei in the same system to probe different regions in q space of $\chi(q, \omega)$. In Hg1201 one has $A(q_{\text{AF}}) = 0$ for the hyperfine interaction of ¹⁹⁹Hg nucleus with the Cu moments provided that the Cu electronic spins are antiferromagnetically (AF) correlated at $q = q_{\text{AF}}$ both within a given CuO₂ plane and between adjacent planes. Hence, the ¹⁹⁹Hg is a good microscopic probe of the response of the electronic system at $q=0$ just as ⁸⁹Y is in YBa₂Cu₃O₇ (Y123) and Y-based HTSC. ¹⁹⁹Hg has the noticeable advantage over ⁸⁹Y NMR of a larger nuclear moment and a larger hyperfine coupling constant. For ⁶³Cu one can use the model Hamiltonian adopted to analyze Knight shift and spin-lattice relaxation¹² and write for the filtering factors $A(q)$ in Eq. (5)

$$A(q)|_{H||c} = A_{\perp} + 2B[\cos(q_x a) + \cos(q_y a)], \quad (6)$$

where A_{\perp} is the on-site anisotropic coupling tensor, while B is the isotropic transferred hyperfine coupling for each of four nearest-neighbor Cu spins which are assumed to be correlated. Equation (6) shows that unless $A_{\perp} \sim 4B$, the ⁶³Cu site is sensitive to enhancement of the generalized spin susceptibility at the antiferromagnetic wave vector $q_{\text{AF}} = \pi/a$.

If one models the generalized susceptibility $\chi(q, \omega)$ (Ref. 13) for the highly correlated electronic system then the NSLR can yield useful information through Eq. (5). One of the main issues in HTSC is whether the Fermi liquid of doped oxygen holes and the Cu d electrons form a single-spin fluid described by a unique spin susceptibility $\chi(q, \omega)$ or by the sum of two independent contributions: $\chi(q, \omega) = \chi_0(q, \omega) + \chi_{\text{AF}}(q, \omega)$. In either case the Cu spins which are strongly coupled by an antiferromagnetic (AF) exchange interaction are expected to give rise to an enhanced susceptibility for $q = q_{\text{AF}}$.

In the presence of a weakly interacting Fermi gas and for a direct contact and/or dipolar hyperfine interaction of the conduction electrons with the nucleus the expression in Eq. (5) reduces to the Korringa relation⁹

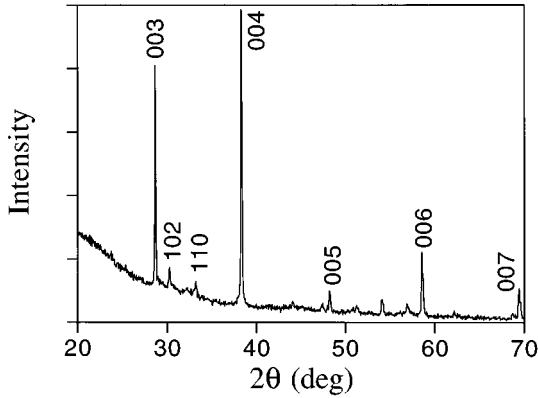


FIG. 1. X-ray-diffraction pattern of an optimally oxygen-doped $\text{HgBa}_2\text{CuO}_{4+\delta}$ powder sample with grains aligned with a common crystallite c axis.

$$K^2 T_1 T = S, \quad (7)$$

$$S = \frac{h}{8\pi^2 k_B} \left(\frac{\gamma_e}{\gamma_N} \right)^2,$$

where γ_e is the gyromagnetic ratio of a free electron and γ_N is the nuclear gyromagnetic ratio. The T and K dependence of T_1^{-1} are found to be described by Eq. (7) also for a correlated and strongly interacting Fermi gas provided that the orbital contribution to NSLR is negligible and that one uses in Eq. (7) only the spin contribution to the total shift, $K^{\text{sp}}(T)$. However, in the presence of interactions and of correlations among conduction electrons the so-called Korringa ratio, i.e., $K^2 T_1 T / S$ may be found to be quite different from unity.^{1,9}

III. EXPERIMENTAL DETAILS

A. Sample

A single-phase powder sample of optimally oxygen-doped $\text{Hg}1201$ with $T_c = 96$ K was prepared by the method described in detail elsewhere.^{14,15} The powder grains of an average diameter $12\text{--}20$ μm were mixed with a low viscosity and low magnetic susceptibility out-gassed epoxy (EPOTEK 301) in a Teflon container and placed in a magnetic field of 8.2 T for 15 h. A flat-plate sample was prepared for the x-ray-diffraction studies to test whether the c axis of the grain-aligned sample was perpendicular to the surface of the plate. At the same time cylindrical samples with different sizes were made for both magnetization and NMR measurements.

X-ray-diffraction patterns for an aligned sample is shown in Fig. 1 where the enhancement of background intensity at low diffraction angle is from the amorphous epoxy. By comparing the relative intensity of the (003) line with the (102) main line characteristic of the randomly oriented powder,⁶ we could estimate that more than 85% of the grains are aligned with the crystallite c axis along the field. Although the alignment obtained is not perfect, it is sufficient to give detailed information on the orientation dependence of Knight shift and relaxation rates because of the large anisotropy of the Knight shift in the whole temperature range investigated. These data will be shown and discussed in Sec. IV.

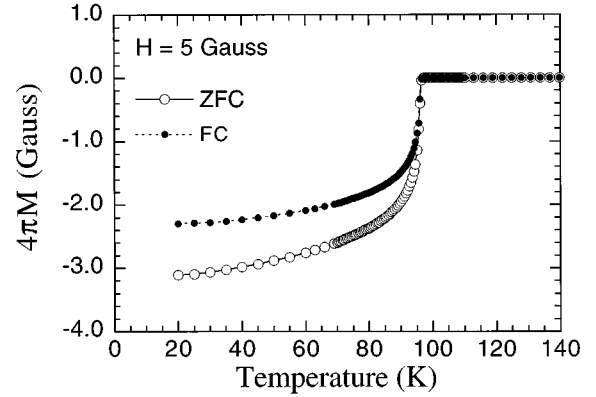


FIG. 2. dc magnetization for $\mathbf{H}||c$ vs temperature for the aligned $\text{HgBa}_2\text{CuO}_{4+\delta}$ sample: (○) zero-field cooled, and (●) field cooled.

The sample quality after alignment was characterized by dc magnetization measurements to test whether the sample has been contaminated in the alignment process or not. As shown in Fig. 2, a sharp superconducting transition was observed for the aligned sample, strongly suggesting that the sample quality was not affected by the alignment process.

B. Measurements

X-ray-diffraction and dc magnetization measurements using Quantum Design superconducting quantum interference device spectrometer were performed to characterize the aligned $\text{Hg}1201$ powder sample. ^{199}Hg and ^{63}Cu NMR measurements were performed in a magnetic field of 8.2 T with a homebuilt coherent Fourier transform (FT) pulse spectrometer¹⁶ operating at 62 and 93 MHz, respectively. Typical $\pi/2$ radio frequency (rf) pulse lengths for ^{199}Hg were 4 μs corresponding to an rf magnetic-field strength of 80 G. The rf field strength was sufficient to cover the whole spectrum with the linewidth less than 60 kHz above 20 K for both orientations. NMR spectra were obtained from the FT of half of the echo signal using typical two-pulse Hahn echo method (TPHE).¹⁷ The spin-echo decay rate T_2^{-1} was moni-

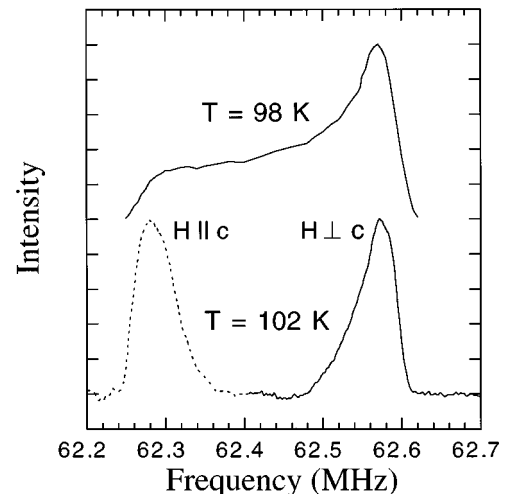


FIG. 3. Representative ^{199}Hg NMR spectra at $H=8.2$ T for a randomly oriented powder sample (upper trace) and for the aligned sample for both orientations; $\mathbf{H}||c$ and $\mathbf{H}\perp c$ (lower trace).

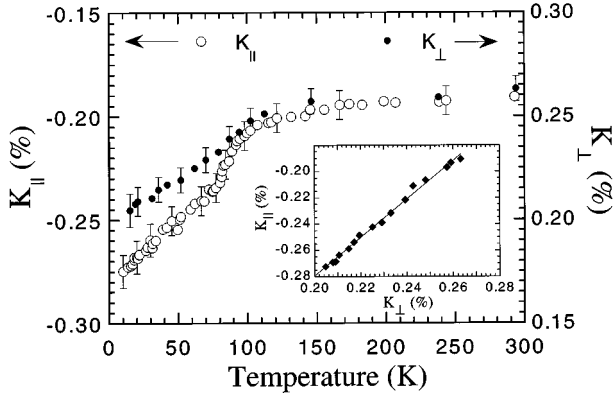


FIG. 4. Temperature dependence of the ^{199}Hg NMR shift for two orientations of the external magnetic field with respect to the tetragonal c axis: (○) K_{\parallel} for $\mathbf{H}\parallel c$, and (●) K_{\perp} for $\mathbf{H}\perp c$. Note the different scales for K_{\parallel} and K_{\perp} . The inset is a plot of K_{\parallel} vs K_{\perp} .

tored with a TPHE sequence $(\pi/2)_x - \tau - (\pi)_y$ with variable τ separation. The nuclear spin-lattice relaxation rate (NSLR, T_1^{-1}) measurements were performed by monitoring the return to thermal equilibrium of the nuclear magnetization with a $\pi/2$ rf pulse after inverting the magnetization with a π rf pulse.¹⁷ The ^{63}Cu NMR measurements were performed only for $\mathbf{H}\parallel c$ where no second-order quadrupole shift of the NMR central line transition ($1/2 \leftrightarrow -1/2$) is present. The ^{63}Cu NSLR was measured from the recovery of the nuclear magnetization following a long saturation sequence. The value of $1/T_1 = 2W$ was obtained from the fitting of the recovery to the law: $[M(\infty) - M(t)]/M(\infty) = C_1 \exp(-2Wt) + C_2 \exp(-12Wt)$ yielding $C_1 \approx 0.45$ and $C_2 \approx 0.55$ in the whole temperature investigated, which are close to the theoretical values $C_1 = 0.4$ and $C_2 = 0.6$.

All measurements were taken in field-cooled conditions with an applied magnetic field of 8.2 T which is much greater than the low critical field H_{c1} , and in the temperature range $10 \text{ K} < T < 300 \text{ K}$ for two crystal orientations with respect to the applied magnetic field: $\mathbf{H}\parallel c$ and $\mathbf{H}\perp c$.

IV. RESULTS

A. ^{199}Hg NMR spectrum and Knight shift (K)

Representative ^{199}Hg NMR spectra in the oriented powder sample are shown in Fig. 3 for both orientations; $\mathbf{H}\parallel c$ and $\mathbf{H}\perp c$, and compared with the powder spectrum obtained from a randomly oriented powder sample of Hg 1201 (Ref. 6) in order to show the good correspondence of the powder pattern features with the oriented powder signals. The signals for the oriented powder are slightly anisotropic revealing the presence of some powder not aligned as indicated also by the

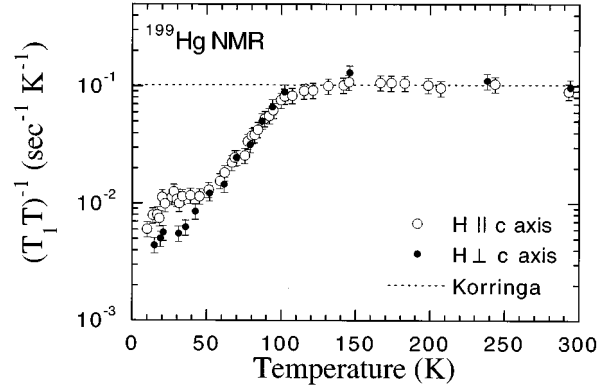


FIG. 5. Temperature dependence of $(T_1 T)^{-1}$ of ^{199}Hg for both orientations of the external magnetic field: (○) $\mathbf{H}\parallel c$, and (●) $\mathbf{H}\perp c$. The dashed line is a fit to a Korringa behavior, $(T_1 T)^{-1} = 0.1 \text{ sec}^{-1} \text{ K}^{-1}$.

x-ray-diffraction pattern in Fig. 1. In spite of the small degree of misalignment of the sample, the large anisotropy of the Knight shift allows for sufficient spectral resolution to measure the orientation dependence of the Knight shifts and the relaxation rates with good accuracy.

The Knight shifts, K_{\parallel} and K_{\perp} , were obtained from the relative frequency shift of the peak positions of the spectra with respect to the ^{199}Hg resonance frequency in an aqueous solution of $\text{Hg}(\text{NO}_3)_2$. The results are shown in Fig. 4 as a function of temperature, while in Table I we give numerical results for three representative temperatures. Both K_{\parallel} and K_{\perp} are found to decrease rapidly below T_c as expected for the superconducting gap opening. An interesting feature for the interpretation of the data is the linear relation between K_{\parallel} and K_{\perp} which holds in the whole temperature range investigated as shown in the inset of Fig. 4. A linear relation between K_{\parallel} and K_{\perp} was previously reported for ^{89}Y NMR in $\text{YBa}_2\text{Cu}_3\text{O}_7$ (Y123).¹⁸

B. ^{199}Hg nuclear spin-lattice relaxation rate (NSLR, T_1^{-1})

The ^{199}Hg nuclear magnetization recovery was found to obey a single exponential law in the whole temperature range investigated. The results for NSLR, T_1^{-1} are shown in Fig. 5 as a plot of $(T_1 T)^{-1}$ vs T for both orientations of the external magnetic field with respect to the tetragonal c axis. The Korringa behavior, $(T_1 T)^{-1} \approx 0.1 \text{ sec}^{-1} \text{ K}^{-1}$, in the normal state and the sharp decrease of $(T_1 T)^{-1}$ below T_c observed here are in good agreement with the preliminary ^{199}Hg NMR measurement performed in the Hg 1201 powder sample.⁶ The absence of a measurable orientation dependence of T_1^{-1} in the normal state is an important result considering the

TABLE I. ^{199}Hg Knight shifts in Hg1201 at three representative temperatures; K^{tot} is the observed total Knight shift and K^{sp} is the spin contribution term extracted by using the Korringa relation. The data below are corrected for the demagnetization effects as discussed in the text.

T (K)	$K_{\parallel}^{\text{tot}}$ (%)	K_{\perp}^{tot} (%)	$K_{\text{iso}}^{\text{tot}}$ (%)	$K_{\text{ax}}^{\text{tot}}$ (%)	$K_{\text{iso}}^{\text{sp}}$ (%)	$K_{\text{ax}}^{\text{sp}}$ (%)
294	-0.19	0.26	0.11	-0.15	0.07	≈ 0.0
102	-0.21	0.25	0.10	-0.15	0.06	≈ 0.0
15	-0.25	0.20	0.05	-0.15	≈ 0.0	≈ 0.0

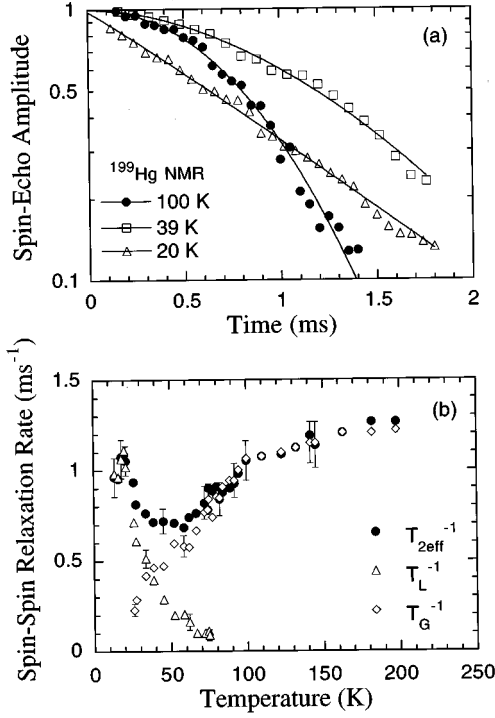


FIG. 6. ^{199}Hg nuclear spin-spin relaxation: (a) Representative decays of the spin-echo amplitude as a function of the pulse separation in a two-pulse Hahn echo experiment. (b) Temperature dependence of the different parameters extracted from the fit of the spin-echo decay: (●) $T_{2\text{eff}}^{-1}$, (△) T_L^{-1} , and (◇) T_G^{-1} (see the text for details).

large anisotropy of K . The measurements reported here are more accurate than the previous powder measurements and allow one to measure a small but detectable deviation from a constant $(T_1T)^{-1}$ starting about 10 K above T_c .

Below T_c the NSLR drops rapidly without any sign of a coherence peak, a common trend in HTSC. An anomalous enhancement of $(T_1T)^{-1}$ can be observed around 30 K for $\mathbf{H}\parallel\mathbf{c}$. The anomaly is explained by an additional relaxation mechanism due to the thermally activated flux motion. A systematic investigation of this effect with measurements at different applied magnetic fields is reported in details elsewhere.⁷

C. ^{199}Hg nuclear spin-spin relaxation rate (T_2^{-1})

The relaxation of the transverse magnetization which is characterized by the spin-spin relaxation rate T_2^{-1} shows an unusual temperature dependence. Above T_c the decay of the transverse nuclear magnetization, $M(t)$ in a TPHE experiment follows a Gaussian law. Below T_c the decay becomes progressively more and more exponential. Some typical decays of the echo amplitude are shown in Fig. 6(a) for the purpose of illustration of the effect. In order to analyze the data we utilized two different methods: the simplest is to define an effective $T_{2\text{eff}}$ from the condition $M(T_{2\text{eff}})/M(0)=1/e$; the second method is to fit the spin-echo decay using the expression¹⁹

$$M(t) = M(0) \exp\left(-\frac{t}{T_L}\right) \exp\left[-\left(\frac{t}{T_G}\right)^2\right]. \quad (8)$$

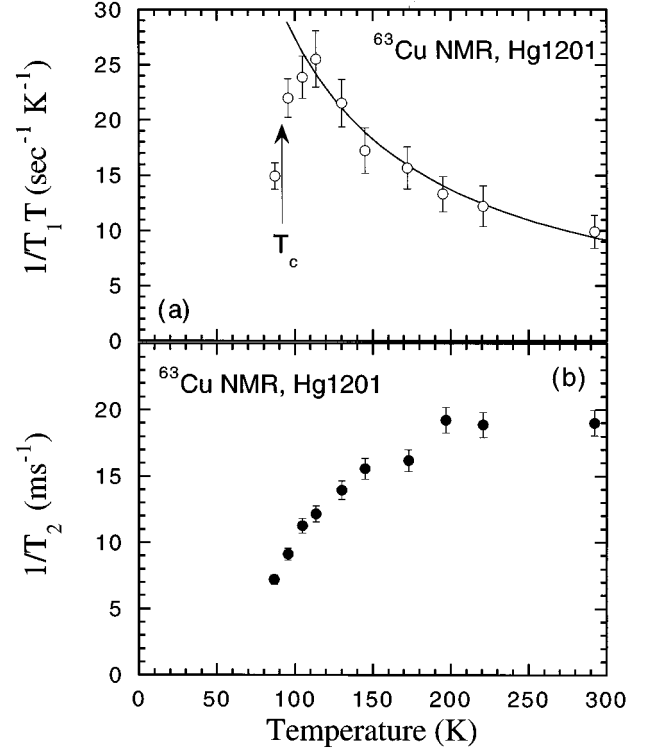


FIG. 7. ^{63}Cu NMR in $\text{HgBa}_2\text{CuO}_{4+\delta}$ for $\mathbf{H}\parallel\mathbf{c}$: (a) $(T_1T)^{-1}$ vs. T . The solid line is a fit to $(T_1T)^{-1} = C/T$ yielding $C = 2740$ K. (b) T_2^{-1} vs. T .

The temperature dependence of $T_{2\text{eff}}^{-1}$ and the two components, T_L^{-1} and T_G^{-1} , of the spin-echo decay are plotted in Fig. 6(b) for ^{199}Hg in Hg1201 for $\mathbf{H}\parallel\mathbf{c}$.

An interesting observation is the anomalous enhancement of T_L^{-1} which has a peak around 20 K. Similar anomalies of T_2^{-1} were already reported for ^{89}Y in Y123 (Ref. 20) and ^{205}Tl in $\text{Tl}_2\text{Ba}_2\text{Ca}_2\text{Cu}_3\text{O}_{10+\delta}$ ²¹ and explained by the effect of thermally activated flux motion. On the other hand, the Gaussian component of the spin-echo decay, i.e., T_G^{-1} , is believed to arise from the ^{199}Hg nuclear magnetic dipolar interaction. Its magnitude and temperature dependence is interpreted in the following section as due to the pseudodipolar interaction via the conduction electrons (holes).

D. ^{63}Cu nuclear spin-lattice ($T_1^{-1} \equiv 2W$) and nuclear spin-spin (T_2^{-1}) relaxation rates

The ^{63}Cu nuclear spin-lattice relaxation rate T_1^{-1} ($\equiv 2W$) was obtained from the recovery law as explained in Sec. III. The ^{63}Cu spin-spin relaxation was found to obey an exponential decay in the whole temperature range investigated from which a single T_2 parameter was measured. The results for the ^{63}Cu $(T_1T)^{-1}$ ($\equiv 2W/T$) and T_2^{-1} are shown Figs. 7(a) and 7(b). As seen in Figs. 7(a) and 7(b), $(T_1T)^{-1}$ increases with decreasing temperature and starts to drop with maximum around 110 K above T_c , while T_2^{-1} decreases monotonically with decreasing temperature. A large ^{63}Cu Knight shift for $\mathbf{H}\parallel\mathbf{c}$ $K_{\parallel} = (1.47 \pm 0.05)\%$ is observed at room temperature and is found to decrease slightly with decreasing temperature yielding $K_{\parallel} = (1.43 \pm 0.05)\%$ at $T \approx 100$ K.

V. DATA ANALYSIS AND DISCUSSION

A. Anisotropy of the ^{199}Hg shift tensor

The ^{199}Hg NMR shift is very anisotropic as is evident from the spectra in Fig. 3. In our previous report⁶ we concluded that the large observed anisotropy originates mostly from the orbital currents induced by the field \mathbf{H} in the linear dumbbell configuration of Hg-O(2) bond.

The NMR data obtained from an oriented Hg1201 sample strongly support the previous conclusion in several ways. The total axial shift $K_{\text{ax}}^{\text{tot}}$ defined in Eq. (3) remains almost constant as $T \rightarrow 0$, as shown in Fig. 4 and Table I, indicating that $K_{\text{ax}}^{\text{tot}}$ is not related to the spin susceptibility. Furthermore it is unlikely that the shift anisotropy can originate from an anisotropy of the temperature-independent Van Vleck (VV) contribution to the magnetic susceptibility. Such an anisotropy would be at least partially reflected in NSLR, T_1^{-1} , behavior which instead is practically isotropic above 50 K as shown in Fig. 5. Finally in order to estimate the contribution to the shift anisotropy from the dipolar interaction of the ^{199}Hg nucleus with the localized Cu magnetic moment, the dipolar field at ^{199}Hg site was calculated by summing over a cube with a side of length 30 times the lattice parameter a of the tetragonal Hg1201 crystal and using the expression for the dipolar field, \mathbf{h} , from the Cu at $r=r_j$ (Ref. 8)

$$\mathbf{h}_j = \frac{3(\langle \boldsymbol{\mu} \rangle \cdot \mathbf{r}_j) \mathbf{r}_j}{r_j^5} - \frac{\langle \boldsymbol{\mu} \rangle}{r_j^3}, \quad (9)$$

$$K_{\text{ax}}^{\text{dip}} = \frac{1}{3} (K_{\parallel}^{\text{dip}} - K_{\perp}^{\text{dip}}) = \frac{1}{3} \frac{\sum_j h_{\parallel,j} - \sum_j h_{\perp,j}}{H},$$

where $\langle \boldsymbol{\mu} \rangle$ is the thermal average of the paramagnetic moment of the Cu ion induced by the applied field \mathbf{H} . Assuming an isotropic susceptibility per atom $\chi = \langle \boldsymbol{\mu} \rangle / H = 4 \times 10^{-28}$ (Ref. 6) and from the known Hg-Cu distance, $d = 4.76 \text{ \AA}$,⁵ one has $K_{\text{ax}}^{\text{dip}} = 2.4 \times 10^{-3} \%$. This value is almost two orders of magnitude smaller than the measured value and has the opposite sign (see Table I). Thus we conclude the large observed shift anisotropy should be ascribed almost entirely to the anisotropic chemical shift originating from the linear configuration of the Hg-O(2) bond.

Now we discuss the correction for the demagnetization effects. As seen in the inset of Fig. 8, the anisotropic ^{199}Hg Knight shift K_{ax} is T independent above T_c and it has a small but rapid decrease by about 0.01% as $T \rightarrow 0$ K. The effect can be ascribed entirely to the contribution to the Knight shift due to the demagnetization effects. From Eq. (3) and (4) one has

$$K_{\text{ax}}^{\text{meas}}(T) = K_{\text{ax}}^{\text{orb}} + \frac{4\pi}{3H} [(1 - N_{\parallel})M_{\parallel}(T) - (1 - N_{\perp})M_{\perp}(T)]. \quad (10)$$

In the weakly anisotropic HTSC $\text{YBa}_2\text{Cu}_3\text{O}_7$, one has $M_{\parallel}/M_{\perp} \cong 5$. In our anisotropic system the ratio of the magnetizations should be even larger. Thus we can assume $M_{\perp}(T) \ll M_{\parallel}(T)$ and neglect the second term in the parenthesis of Eq. (10). The temperature dependence of the magnetization for $H_{c1} \ll H \ll H_{c2}$ can be expressed as²²

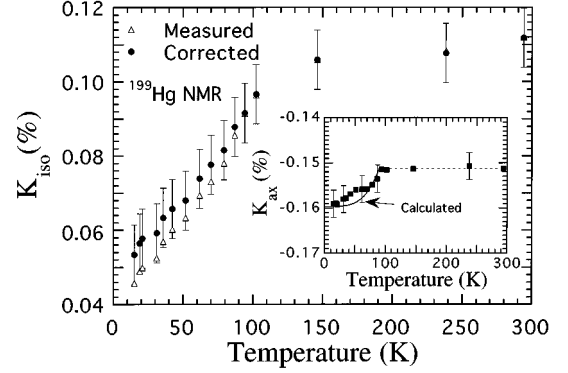


FIG. 8. Plot of the temperature dependence of the ^{199}Hg isotropic Knight shift K_{iso} component as measured and after corrected for the effects of the diamagnetic shielding below T_c . The inset shows the temperature dependence of the anisotropic Knight shift K_{ax} component and the calculated behavior due to the anisotropic shielding effects below T_c (see text for details).

$$4\pi M_{\parallel}(T) = -\frac{\Phi_0}{8\pi\lambda_{\parallel}^2(T)} \ln\left(\frac{H_{c2}}{H}\right), \quad (11)$$

where $\Phi_0 = 2.07 \times 10^{-7} \text{ G cm}^2$ is the quantum of flux, $\lambda_{\parallel}(T)$ is the penetration length and H_{c2} is the upper critical field. By assuming $H_{c2} = 75 \text{ T}$, $\lambda_{\parallel}(0) = 1500 \text{ \AA}$ one can estimate from Eqs. (10) and (11) the correction term $\Delta K_{\text{ax}}^M(T=0) = -0.033(1 - N_{\parallel})\%$ for $H = 8.2 \text{ T}$ which agrees with the experimental value -0.01% for $N_{\parallel} = 0.70$. Using the temperature dependence of λ , $\lambda^2(T) = \lambda^2(0)[1 - (T/T_c)^4]^{-1}$ and from Eqs. (10) and (11), one can calculate the temperature dependence of the contribution of the demagnetization effects to K_{ax} . The calculated values are compared with the experimental ones in the inset of Fig. 8. The lack of detailed agreement can be easily explained due to the possible deviation of $\lambda_{\parallel}(T)$ from the temperature dependence expected from the two-fluid model and/or due to the experimental error in the determination of K_{ax} . However, it is quite clear that the entire T dependence of K_{ax} below T_c can be ascribed to the demagnetization effects. Thus we use now the correction obtained from the T dependence of K_{ax} to correct the $K_{\text{iso}}(T)$ data. We write

$$K_{\text{iso}}^{\text{meas}}(T) = K_{\text{iso}}^{\text{orb}} + K_{\text{iso}}^{\text{sp}}(T) + \frac{4\pi}{3H} [(1 - N_{\parallel})M_{\parallel}(T) + 2(1 - N_{\perp})M_{\perp}(T)]. \quad (12)$$

By assuming $M_{\perp}(T) \ll M_{\parallel}(T)$ and $(4\pi/3H)[(1 - N_{\parallel})M_{\parallel}(T)] \cong \Delta K_{\text{ax}}(T)$ (i.e., assuming the temperature dependence of K_{ax} is totally ascribed to the demagnetization effects) we obtain the intrinsic $K_{\text{iso}}(T)$ corrected for the demagnetization effects. Figure 8 shows the corrected data together with the measured $K_{\text{iso}}^{\text{meas}}(T)$. The correction has uncertainties due to the lack of knowledge of the exact magnetization $\mathbf{M}(T)$ and of the demagnetization factor N for the two orientations in this Hg1201 oriented powder.

In addition, the experimental observation of a negligible anisotropy of T_1^{-1} , $1 \leq T_{1,\perp}^{-1}/T_{1,\parallel}^{-1} \leq 1.1$ in the normal state, (see Fig. 5) is consistent with a negligible contribution to the

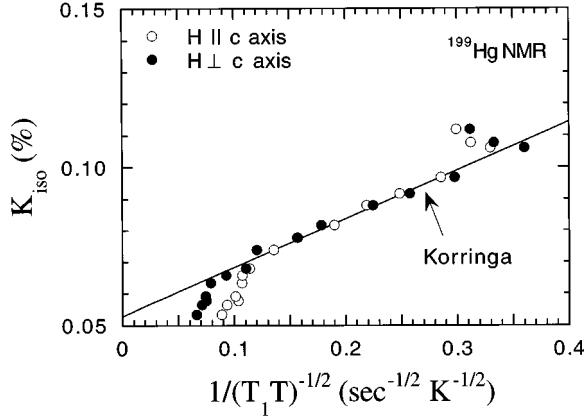


FIG. 9. Plot of the ^{199}Hg NMR shifts K_{iso} vs $(T_1 T)^{-1/2}$: (○) $\mathbf{H} \parallel \mathbf{c}$ and (●) $\mathbf{H} \perp \mathbf{c}$. The line is a fit to find the T -independent $K_{\text{iso}}^{\text{orb}}$ using the Korringa relation; $K_{\text{iso}}(T) = 0.053 + 0.155(T_1 T)^{-1/2}$. The data are corrected for the demagnetization effects.

anisotropic Knight shift from terms related to the spin susceptibility and/or to the Van Vleck T -independent susceptibility.

B. ^{199}Hg Knight shift and NSLR

The observation of the Korringa behavior $(T_1 T)^{-1} = \text{const} \cong 0.1 \text{ sec}^{-1} \text{ K}^{-1}$ and the observation of negligible anisotropy of T_1^{-1} in the normal state suggest that the ^{199}Hg T_1^{-1} probes the Fermi-liquid behavior at $q=0$ through the isotropic contact hyperfine interaction without additional contributions coming from AF fluctuations at $q=q_{\text{AF}}$. This is consistent with the point symmetry of Hg nucleus which implies the filtering of AF fluctuations of the Cu spins for three-dimensional (3D) correlation of the spins. The simple Korringa relation [Eq. (7)] is valid for a weakly interacting Fermi gas. For a highly correlated Fermi liquid the proportionality of $(T_1 T)^{-1}$ to K^2 may still be valid if the NSLR is dominated by the uniform ($q=0$) generalized susceptibility. In order to verify this point we plot of K_{iso} vs $(T_1 T)^{-1/2}$ in Fig. 9 where K_{iso} are corrected for demagnetization effects as discussed above. The K_{iso} appears to scale linearly to $(T_1 T)^{-1/2}$ for a wide temperature range including the superconducting and the normal states ($50 \text{ K} < T < 250 \text{ K}$). The deviation at high temperature ($T > 250 \text{ K}$) may be due to a decrease of the filtering effect at the Hg site reflecting the decrease of 3D correlation of the AF fluctuations with increasing temperature or simply due to a sample inhomogeneity. The deviation at low temperature ($T < 50 \text{ K}$) can be explained by an additional relaxation mechanism in the vortex state⁷ which is not an intrinsic property of the normal Fermi liquid. Thus, by assuming $(T_1 T)^{-1/2} \propto K_{\text{iso}}^{\text{sp}}(T) = K_{\text{iso}}(T) - K_{\text{iso}}^{\text{orb}}$ and $K_{\text{iso}}^{\text{sp}}(T=0) = 0$, the temperature-independent term $K_{\text{iso}}^{\text{orb}}$ can be obtained by extrapolation to $(T_1 T)^{-1/2} = 0$ as $T \rightarrow 0$. We find $K_{\text{iso}}^{\text{orb}} = 0.053\%$ yielding $K_{\parallel}^{\text{orb}} = -0.25\%$ and $K_{\perp}^{\text{orb}} = +0.20\%$ by combining with $K_{\text{ax}}^{\text{orb}} = -0.15\%$. The spin contribution to the Knight shift $K_{\text{iso}}^{\text{sp}}$ can be obtained by subtracting the above estimates for $K_{\text{iso}}^{\text{orb}}$ from the total Knight shift.

In Table I, the values of K^{sp} are shown for representative temperatures. This analysis (especially for $K_{\text{ax}}^{\text{sp}}$) may include

considerable uncertainties since we obtained the relatively small value of $K_{\text{ax}}^{\text{sp}}$ by subtracting a large value of $K_{\text{ax}}^{\text{orb}}$ from the total shift. Using the estimated $K_{\text{iso}}^{\text{sp}}$, one obtains a Korringa value, $K_{\text{iso}}^2 T_1 T \cong 0.25 \times 10^{-5} \text{ sec K}$ in the temperature range $50 \text{ K} < T < 250 \text{ K}$. If we define the Korringa ratio κ as⁹

$$\kappa \equiv \frac{K^2 T_1 T}{S}, \quad (13)$$

where $S = 0.83 \times 10^{-5} \text{ sec K}$ for ^{199}Hg [see Eq. (7)], we obtain $\kappa \cong 0.31$ for ^{199}Hg in Hg1201. This can be compared with the value of $\kappa = 1.1$ derived for ^{199}Hg in Hg metal.²³ The Korringa ratio obtained here for ^{199}Hg in Hg1201, $\kappa \cong 0.31$, is not too far from the values quoted above for the simple Hg metal thus confirming that the ^{199}Hg NSLR is dominated by the coupling with the normal Fermi liquid without additional enhancements due to AF fluctuations. It is noted that the effect of ferromagnetic interactions among conduction electrons which is responsible for the Stoner enhancement of the uniform spin susceptibility would lead to a Korringa ratio greater than one, $\kappa > 1$.⁹ In Hg1201 the deviation of the Korringa ratio is in opposite direction, i.e., $\kappa < 1$. This can be easily explained by the presence in $K_{\text{iso}}^{\text{sp}}$ of a small negative term arising from the exchange polarization of s electrons by $\text{Cu } d$ electrons⁹ (as expected for the single-spin fluid).

We conclude the ^{199}Hg K and T_1 are related by the Korringa relation with a value of the Korringa ratio close to one as for normal metals. Based on the above conclusion that ^{199}Hg NMR is a good probe to study the behavior of the Fermi liquid in Hg1201, we will discuss the properties of the Fermi liquid both in the normal and in the superconducting state in the following paragraphs.

C. Temperature dependence of the spin susceptibility from ^{199}Hg K and T_2

As shown in the previous paragraph the analysis of the temperature dependence of $(T_1 T)^{-1}$ and of the Knight shift allows one to separate the component related to the uniform spin susceptibility $\chi'(0,0)$ of the Fermi liquid from the total shift. The temperature dependence of $K_{\text{iso}}^{\text{sp}}(T)$, which measures the temperature dependence of $\chi'(0,0)$, is shown in Figs. 10 and 11.

Before discussing the temperature dependence of $K_{\text{iso}}^{\text{sp}}(T)$ we would like to reconsider the results of the nuclear spin-spin relaxation rate. As discussed in Sec. III C the echo amplitude decay curve can be fit as the product of a Gaussian decay characterized by a time constant T_G and an exponential one with a time constant T_L . For $T > 50 \text{ K}$ the Gaussian component is dominant as shown in Fig. 6. At room temperature $T_G^{-1} = 1.2 \text{ ms}^{-1}$. This value is considerably larger than the value $(T_G^{-1})_{\text{dip}} \approx 0.2 \text{ ms}^{-1}$ which can be estimated from a direct nuclear dipolar interaction among ^{199}Hg nuclei. We stress that only the homonuclear dipolar interaction contributes to the TPHE decay.⁸ Thus we argue that the echo decay is dominated by an indirect nuclear interaction. This is not surprising since ^{199}Hg has a very large hyperfine coupling constant. The indirect nuclear interaction can be either a pseudoexchange interaction of the form $A_{12} \mathbf{I}_1 \cdot \mathbf{I}_2$ or a pseudodipolar interaction of the form $B_{12} [\mathbf{I}_1 \cdot \mathbf{I}_2 - 3(\mathbf{I}_1 \cdot \mathbf{R}_{12})(\mathbf{I}_2 \cdot \mathbf{R}_{12})/R_{12}^2]$.⁸ The importance of these indirect interactions in heavy metals and insulators was well

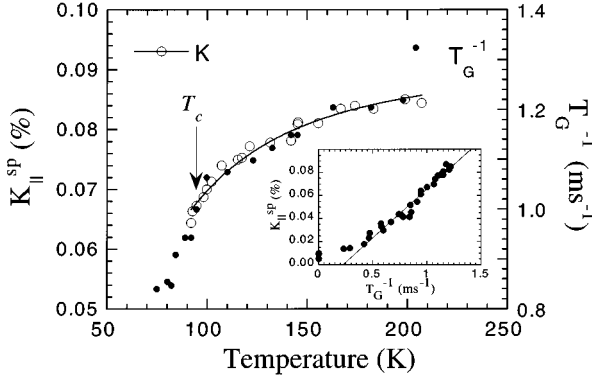


FIG. 10. Temperature dependence of the ^{199}Hg Knight shift and of the Gaussian component of the spin-spin relaxation rate: (○) $K_{\parallel}^{\text{sp}}$, and (●) T_G^{-1} . The solid line is a fit of $K_{\parallel}^{\text{sp}}$ by Eq. (14) in the text with the fitting parameters; $K_0=0.09\%$ and $\Delta_{\text{sp}}=106$ K. The inset is a plot $K_{\parallel}^{\text{sp}}$ vs T_G^{-1} .

documented in the pioneering works by Bloembergen and Rowland²⁴ and Ruderman and Kittel.²⁵

In the present case the indirect interaction of the ^{199}Hg nuclei is mediated by the Fermi liquid of oxygen holes and is expected to be equivalent to the pseudodipolar interaction in Tl and Hg metals.⁹ In simple metals one expects that the pseudoexchange interaction constant A_{12} behaves as a function of internuclear distant R as $(\sin 2k_F R - 2k_F R \cos 2k_F R)/R^4$, where k_F is the conduction-electron wave vector at the Fermi level.⁸ The expression for the pseudodipolar interaction B_{12} is more complicated and is related to the non- s components of the wave function of the conduction electrons.²⁴ In the inset of Fig. 10 we show that the spin component of the Knight shift appears to be directly proportional to T_G^{-1} . This observation suggests that the indirect pseudoexchange and/or pseudodipolar interaction is simply proportional to the uniform spin susceptibility $\chi'(0,0)$. This conclusion is not surprising since the form of the indirect interaction discussed above is asymptotically proportional to k_F and hence to $\chi'(0,0)$.

It should be emphasized that the Gaussian component in the spin-echo decay of $^{63,65}\text{Cu}$ in Y123 and other HTSC discussed by Pennington and Slichter²⁶ has the same origin as the pseudoexchange interaction discussed above as implicitly recognized in a later work by Imai *et al.*²⁷ While for $^{63,65}\text{Cu}$ and for $\mathbf{H}\parallel\mathbf{c}$ the indirect nuclear interaction is proportional to the generalized susceptibility at $q=q_{\text{AF}}$ as a consequence of the enhancement of $\chi'(q_{\text{AF}},0)$ due to AF fluctuations and of the form of the filtering factors $A(q)$ [see Eq. (5)], for ^{199}Hg the indirect nuclear coupling is proportional to $\chi'(0,0)$ making the ^{199}Hg nucleus an ideal probe of the Fermi-liquid behavior.

As shown in Fig. 10 both $K_{\parallel}^{\text{sp}}$ and T_G^{-1} decrease with decreasing temperature starting well above T_c . Both the effects on T_G^{-1} and on K must arise from a decrease of the spin susceptibility χ^{sp} . The decrease of χ^{sp} as evidenced by K^{sp} is rather common phenomena in HTSC except for the overdoped Y123 and has been attributed to the opening of a gap on the spin-excitation spectrum, so-called a spin pseudogap. Although the origin of the spin pseudogap is still under debate,^{3,28,29} the phenomenological description of the temperature dependence for both static and dynamic spin sus-

ceptibility seems to have a common ground.¹ Thus we tried to fit the ^{199}Hg NMR Knight-shift data to the phenomenological expression given by

$$K(T) = K_0 \left[1 - \tanh^2 \left(\frac{\Delta_{\text{sp}}}{2T} \right) \right], \quad (14)$$

where the fitting parameter Δ_{sp} is the apparent spin-gap energy at $q=0$ and K_0 is the constant value at high temperature. As shown in Fig. 10, the experimental K^{sp} values are found to fit well to the Eq. (14) and the fitting value $\Delta_{\text{sp}}=106$ K is close to the temperature at which $(T_1 T)^{-1}$ starts to decrease.

One can envisage two possible explanations for the decrease of $\chi'(0,0)$ above T_c . The decrease can be the consequence of the transfer of spectral weight of the excitations from low frequency to high frequency. This is the dynamical spin pseudogap at $q=0$ discussed in the literature. On the other hand, a decrease of $\chi'(0,0)$ could be simply the consequence of the transfer of intensity in the generalized susceptibility $\chi'(q,0)$ from $q=0$ to $q=q_{\text{AF}}$ as result of the enhancement of AF fluctuations provided that the sum rule $\chi'(q,0)=\text{constant}$ is valid even for the system of nonlocalized magnetic moments.³⁰ The issue of the opening of a spin pseudogap in our sample appears to be of relevance since the Hg 1201 used here is optimally doped ($T_c=96$ K) and no decrease of $\chi'(0,0)$ above T_c was observed in optimally doped Y123.

D. Antiferromagnetic fluctuations and spin pseudogap from ^{63}Cu relaxation

The linear temperature dependence of T_1^{-1} for ^{199}Hg led us to conclude in Sec V B that the antiferromagnetic fluctuations of the Cu^{2+} spins are correlated between adjacent planes for $T<300$ K implying a strong AF coupling between CuO_2 layers which may seem surprising in this single layer material. In order to verify if strong AF fluctuations are indeed present we performed the NSLR measurements on ^{63}Cu shown in Fig. 7. The ^{63}Cu T_1^{-1} ($\equiv 2W$) is practically constant in the range $110 \text{ K} < T < 300 \text{ K}$ resulting in the Curie-type behavior of $(T_1 T)^{-1}$ shown Fig. 7(a). If the generalized spin susceptibility is strongly peaked at $q_x=q_y=\pi/a$ one expects for $\mathbf{H}\parallel\mathbf{c}$ from Eqs. (5) and (6),

$$\left(\frac{1}{T_1 T} \right) \cong (A_{\perp} - 4B)^2 \chi'(q_{\text{AF}},0) J(q_{\text{AF}},0), \quad (15)$$

where we have assumed $\omega_0 \approx 0$ and have partitioned the dynamical susceptibility $\chi''(q,\omega)/\omega$ in a static part $\chi'(q,0)$ and a dynamical spectral density function $J(q,\omega)$.^{31,32} The enhancement of $(T_1 T)^{-1}$ in the normal state observed in Fig. 7(a) is the clear signature of the enhancement of the AF fluctuations, i.e., $\chi'(q_{\text{AF}},0)$ in Eq. (15). It is noted that the ^{63}Cu Knight shift is practically constant in the normal state and thus it cannot be responsible for the enhancement of $(T_1 T)^{-1}$.

The maximum present in $(T_1 T)^{-1}$ vs T at temperatures higher than T_c [see Fig. 7(a)] is ascribed to the opening of a spin pseudogap. Qualitatively the effect is the result of a competition between the enhancement of $\chi'(q_{\text{AF}},0)$ and a reduction of $J(q_{\text{AF}},0)$ due to the shift of spectral weight from low frequencies to higher frequencies. The maximum in

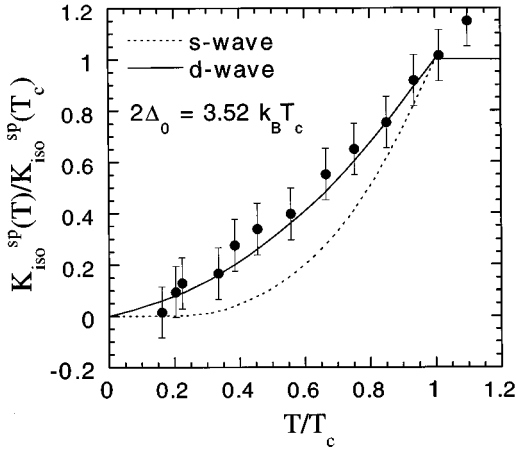


FIG. 11. Plot of the normalized ^{199}Hg Knight shift in the superconducting state: $K_{\text{iso}}^{\text{sp}}(T)/K_{\text{iso}}^{\text{sp}}(T_c)$ vs reduced T/T_c . The lines are theoretical behaviors predicted for s -wave pairing (dashed line) and d -wave pairing (solid line) with the same superconducting gap parameter $2\Delta_0=3.5k_B T_c$ (Ref. 36). The $K_{\text{iso}}^{\text{sp}}(T)$ data are corrected for the demagnetization effects.

$(T_1 T)^{-1}$ of ^{63}Cu should be related to the reduction of ^{199}Hg NMR parameters K and T_G^{-1} (Fig. 10) and $(T_1 T)^{-1}$ (Fig. 5) starting above T_c . Since the ^{199}Hg NMR parameters are sensitive to the uniform susceptibility $\chi'(0,0)$ one could conclude that the opening of the spin pseudogap involves both the $q=0$ and $q=q_{\text{AF}}$ components of the spin-excitation spectrum.

We turn now to a brief discussion of the ^{63}Cu T_2^{-1} data shown in Fig. 7(b). In other CuO_2 -based high- T_c superconductors, for $\mathbf{H} \parallel \mathbf{c}$, it is found that the spin-echo decay has both an exponential and a Gaussian component whereby the latter is related to the static susceptibility at $q=q_{\text{AF}}$, i.e., $\chi'(q_{\text{AF}},0)$.^{19,26,27,29} In the present case we found that the spin-echo decay is dominated by the exponential component with no detectable Gaussian component. An exponential spin-echo decay is also found in other CuO_2 -based HTSC for $\mathbf{H} \perp \mathbf{c}$ and the different echo decay for the two orientations is explained by the anisotropy of the on-site coupling tensor A in the coupling Hamiltonian Eq. (6).¹⁹ Thus one may argue the exponential decay observed in Hg1201 for $\mathbf{H} \parallel \mathbf{c}$ is a consequence of different values of the A tensor due to the presence of apical oxygen. The exponential component is related to nonsecular spin-flip terms in the Hamiltonian and/or to T_1 type of processes involving longitudinal rather than transverse (with respect to the external magnetic field) components of the local field at the ^{63}Cu site at zero frequency.^{8,19} Thus we believe that the reduction of T_2^{-1} reported in Fig. 7(b) starting well above T_c should not be necessarily related to the pseudogap opening. It is pointed out that effects of anisotropy in the fluctuations of the Cu^{2+} spin components could arise as a consequence of deviations of the spin system from the perfect Heisenberg model occurring on lowering temperature. Crossover effects of the Cu^{2+} spin dynamics from Heisenberg to a XY -like correlation have been recently reported in the planar Cu system $\text{Sr}_2\text{CuO}_2\text{Cl}_2$ as $T \rightarrow T_N=256$ K.³³ The presence of similar effects in the Cu planes of high- T_c superconductors should not be ruled out. A more detailed study of ^{63}Cu T_2 and T_1 as a function of temperature

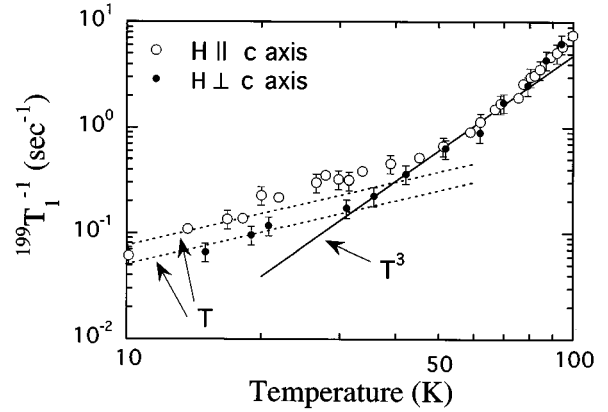


FIG. 12. Log-log plot of ^{199}Hg T_1^{-1} vs T in the superconducting state for both orientations: (○) $\mathbf{H} \parallel \mathbf{c}$ axis and (●) $\mathbf{H} \perp \mathbf{c}$ axis. Lines are fits for T^3 dependence (solid line) and linear- T dependence (dashed lines).

and crystal orientation are necessary before attempting a quantitative analysis of the T_2 data.

E. Symmetry of the pairing state

Here we analyze the ^{199}Hg Knight-shift and NSLR data by comparing their temperature dependence below T_c with theoretical predictions obtained for both s -wave and d -wave gaps.³⁴ In Fig. 11 we plot the normalized value of the spin contribution to the Knight shift which should be a direct measure of the normalized spin susceptibility, i.e., $\chi_s^{\text{sp}}(0,0)/\chi_n^{\text{sp}}(0,0)$ where the subscripts s and n refer to the superconducting and normal state, respectively. The decrease of $^{199}K(T)$ below T_c depends mainly on the size of the superconducting gap $\Delta(T)$ and on the symmetry of the pairing state. However, as has been shown recently by Sudbø *et al.*³⁵ the temperature dependence of K are influenced by details of the Fermi-liquid theory thus making the conclusions of the analysis of the NMR data less straightforward.

In spite of the shortcomings we would like to point out some features of our ^{199}Hg NMR data which seem to support d -wave symmetry for the pairing state. Since no detailed calculations are available for our Hg1201 system we utilize the calculations performed for Y123 by Bulut and Scalapino³⁶ with a BCS value for the gap parameter $2\Delta_0=3.5k_B T_c$ chosen to agree with recent direct tunneling measurements at $T=4.2$ K.³⁷ As shown in Fig. 11 the experimental data are in much better agreement with the slower decrease of $K(T)$ with decreasing temperature predicted for a d -wave gap. However, the tunneling measurements in polycrystalline Hg 1201 (Ref. 37) yielded a range of gaps Δ from ~ 5 to 20 meV, the origin of the spread being unknown. Thus it is conceivable that our Knight-shift data could also be found to be consistent with ab anisotropic s -wave gap as shown for the NMR data in Y123.³⁵

The temperature dependence of the ^{199}Hg spin-lattice relaxation rate T_1^{-1} shown in Fig. 12, is also consistent with the d -wave pairing which predicts a T^3 temperature dependence of the NSLR below T_c .³⁸ As for the case of the Knight shift discussed above, the conclusion for T_1^{-1} is also somewhat ambiguous due to the narrow temperature range in which the

T^3 dependence is observed. The deviation from the T^3 dependence for $T < 40$ K and $\mathbf{H} \parallel \mathbf{c}$ is due to an extra contribution due to the vortex thermal motions not present for $\mathbf{H} \perp \mathbf{c}$.⁷ The deviations from the T^3 dependence for $T < 20$ K and $\mathbf{H} \perp \mathbf{c}$ could be due to a nonzero residual density of states associated with lines of nodes in the gap function.^{39,40}

VI. SUMMARY AND CONCLUSIONS

We have presented the ¹⁹⁹Hg and ⁶³Cu NMR shift and relaxation rate data for a superconducting Hg1201-oriented powder sample. The analysis of both sets of data allows one to reach some conclusions about the electronic properties in the normal state: (i) From ⁶³Cu T_1^{-1} vs T we find evidence for strong antiferromagnetic (AF) fluctuations in the CuO₂ plane; on the other hand ¹⁹⁹Hg T_1^{-1} vs T results do not show evidence of AF fluctuations. If one assumes a single spin-fluid generalized response function this result implies filtering of the AF fluctuations at the Hg site as expected for 3D correlation of the Cu²⁺ moments. Deviations of ¹⁹⁹Hg $(T_1 T)^{-1}$ from a constant above room temperature could be an indication of a crossover from 3D to 2D AF correlations, an issue which is currently explored in Hg1201 and in other Cu-based HTSC. (ii) There is evidence for the opening of a spin pseudogap both at $q=0$ and $q=q_{AF}$ which bears more resemblance with the results in underdoped HTSC than in the optimally doped ones.

We find that the ¹⁹⁹Hg NMR is a good probe of the Fermi-liquid behavior. Both the temperature dependence of the ¹⁹⁹Hg Knight shift and the NSLR below T_c are consistent with a superconducting state characterized by d -wave pairing

with a gap parameter close to the BCS value, i.e., $2\Delta_0 = 3.5k_B T_c$.

As a result of the ¹⁹⁹Hg spin-spin relaxation analysis we find the unexpected result that the Gaussian component of the spin-echo decay, yielding T_G^{-1} , is dominated by a nuclear indirect interaction via the charge carriers. Thus T_G^{-1} can be used to measure directly the uniform spin susceptibility $\chi'(0,0)$ of the Fermi liquid. Considering that all Hg-based compounds, HgBa₂Ca_{*n*-1}Cu_{*n*}O_{2*n*+2+ δ} , have only one Hg site and that the critical temperature T_c is very sensitive to the number of the CuO₂ layers and to the oxygen content δ , the fact that ¹⁹⁹Hg is a good probe to study the Fermi-liquid behavior encourages one to extend the ¹⁹⁹Hg NMR study systematically in Hg-based HTSC with a different number of CuO₂ layers and oxygen content δ .¹⁴

ACKNOWLEDGMENTS

We thank A. Rigamonti, M. Corti, P. Carretta, M. Mali, R. Stern, M. Horvatić, and C. Berthier for helpful discussions. Ames Laboratory is operated for U.S. Department of Energy by Iowa State University under Contract No. W-7405-Eng-82. This work at Ames Laboratory was supported by the Director for Energy Research, Office of Basic Energy Sciences. This work at the University of Arkansas is supported by NSF DMR 9318946, DARPA (Contract No. MDA 972-90-J-1001) through the Texas Center for Superconductivity at the University of Houston (TCSUH). This work at TCSUH is supported by NSF Grant No. 91-22043, USAFOSR Grant No. F49620-93-1-0310 by BMDO, EPRI RP-8066-04, the State of Texas through TCSUH, and the T. L. Temple Foundation.

* Also at Dipartimento di Fisica "A. Volta," Università di Pavia, I-27100 Pavia, Italy.

[†] Present address: New Material Laboratory, Samsung Advanced Institute of Technology, Suwon 440-600, Kyung Ki-Do, Korea.

¹ M. Mehring, Appl. Magn. Reson. **3**, 383 (1992).

² F. Borsa, P. Carretta, M. Corti, and A. Rigamonti, Appl. Magn. Reson. **3**, 509 (1992).

³ D. Brinkmann and M. Mali, in *NMR-Basic Principles and Progress*, edited by P. Diehl, E. Fluck, H. Gunther, R. Kosfeld, and J. Seelig, (Springer-Verlag, Berlin, 1994), Vol. 31, p.171.

⁴ F. Borsa, P. Carretta, F. Cintolesi, M. Corti, A. Rigamonti, B. J. Suh, and D. R. Torgeson, Appl. Magn. Reson. **9**, 149 (1995).

⁵ J. L. Wagner, P. G. Radaelli, D. G. Hinks, J. D. Jorgensen, J. F. Mitchell, B. Dabrowski, G. S. Knapp, and H. A. Beno, Physica C **210**, 447 (1993).

⁶ B. J. Suh, F. Borsa, Ming Xu, D. R. Torgeson, W. J. Zhu, Y. Z. Huang, and Z. X. Zhao, Phys. Rev. B **50**, 651 (1994).

⁷ B. J. Suh, F. Borsa, J. Sok, D. R. Torgeson, M. Corti, A. Rigamonti, and Q. Xiong, Phys. Rev. Lett. **76**, 1928 (1996).

⁸ C. P. Slichter, *Principle of Magnetic Resonance*, 3rd ed. (Springer-Verlag, Berlin, 1990).

⁹ G. C. Carter, L. H. Bennett, and D. J. Kahan, *Metallic Shift in NMR* (Pergamon, New York, 1977), Pt. I.

¹⁰ S. E. Barrett, D. J. Durand, C. H. Pennington, C. P. Slichter, T. A. Friedman, J. P. Rice, and D. M. Ginsberg, Phys. Rev. **41**, 6283 (1990).

¹¹ T. Moriya, J. Phys. Soc. Jpn. **18**, 516 (1963).

¹² F. Mila and T. M. Rice, Physica C **157**, 561 (1989).

¹³ A. Millis, H. Monien, and D. Pines, Phys. Rev. B **42**, 167 (1990).

¹⁴ Q. Xiong, Y. Y. Xue, Y. Cao, F. Chen, Y. Y. Sun, J. Gibson, C. W. Chu, L. M. Liu, and A. Jacobson, Phys. Rev. B **50**, 10 346 (1994).

¹⁵ Q. Xiong, Y. Y. Xue, F. Chen, Y. Cao, Y. Y. Sun, L. M. Liu, A. J. Jacobson, and C. W. Chu, Physica C **231**, 233 (1994).

¹⁶ The NMR spectrometer employed a programmable pulse sequencer [D. J. Adduci and B. C. Gerstein, Rev. Sci. Instrum. **50**, 1403 (1979)]; a double-sideband rf switch [D. R. Torgeson and D. J. Adduci (unpublished)]; and a receiver similar to D. J. Adduci, P. A. Hornung, and D. R. Torgeson, Rev. Sci. Instrum. **47**, 1503 (1976), with a quadrature detector.

¹⁷ E. Fukushima and S. B. W. Roeder, *Experimental Pulse NMR* (Addison-Wesley, Reading, MA, 1981).

¹⁸ H. Alloul, A. Mahajan, H. Casalta, and O. Klein, Phys. Rev. Lett. **70**, 1171 (1993).

¹⁹ C. H. Pennington, D. J. Durand, C. P. Slichter, J. P. Rice, E. D. Bukowski, and D. M. Ginsberg, Phys. Rev. B **39**, 274 (1989).

²⁰ B. J. Suh, D. R. Torgeson, and F. Borsa, Phys. Rev. Lett. **71**, 3011 (1993).

²¹ Y.-Q. Song, S. Tripp, W. P. Halperin, L. Tonge, and T. J. Marks, Phys. Rev. B **50**, 16 570 (1994).

²² A. A. Abrikosov, *Fundamentals of the Theory of Metals* (North-Holland, New York, 1988).

²³ F. Borsa and A. Rigamonti, Nuovo Cimento **48**, 194 (1967).

²⁴ N. Bloembergen and T.J. Rowland, Phys. Rev. **97**, 1679 (1955).

²⁵ M. A. Ruderman and C. Kittel, Phys. Rev. **96**, 99 (1954).

²⁶ C. H. Pennington and C. P. Slichter, Phys. Rev. Lett. **66**, 381 (1991).

- ²⁷T. Imai, C. P. Slichter, A. P. Paulikas, and B. Veal, Phys. Rev. B **47**, 9158 (1993).
- ²⁸A. Sokol and D. Pines, Phys. Rev. Lett. **71**, 2813 (1993).
- ²⁹R. Stern, M. Mali, I. Magelschots, J. Roos, D. Brinkmann, J.-Y. Genoud, T. Graf, and J. Muller, Phys. Rev. B **50**, 426 (1994); R. Stern, M. Mali, J. Roos, and D. Brinkmann, Phys. Rev. B **52**, 15 734 (1995).
- ³⁰R. M. White, *Quantum Theory of Magnetism*, 2nd ed. (Springer-Verlag, Berlin, 1983), p. 116.
- ³¹N. Bulut, D. Hone, D. Scalapino, and J. E. Bickers, Phys. Rev. B **41**, 1792 (1990).
- ³²R. E. Walstedt and W. W. Warren, Science **248**, 1082 (1990).
- ³³B. J. Suh, F. Borsa, L. L. Miller, M. Corti, D. C. Johnston, and D. R. Torgeson, Phys. Rev. Lett. **75**, 2212 (1995).
- ³⁴J. Leggett, Rev. Mod. Phys. **47**, 331 (1975).
- ³⁵A. Sudbø, S. Chakravarty, S. Strong, and P. W. Anderson, Phys. Rev. **49**, 12 245 (1994).
- ³⁶N. Bulut and D. J. Scalapino, Phys. Rev. Lett. **68**, 706 (1992).
- ³⁷Jun Chen, J. F. Zasadzinski, K. E. Grey, J. L. Wagner, and D. G. Hinks, Phys. Rev. B **49**, 3683 (1994).
- ³⁸J. A. Martindale, S. E. Barrett, K. E. O'Hara, C. P. Slichter, W. C. Lee, and D. M. Ginsberg, Phys. Rev. B **47**, 9155 (1993).
- ³⁹K. Ishida, Y. Kitaoka, K. Asayama, K. Kadowaki, and T. Mochiku, J. Phys. Soc. Jpn. **63**, 1104 (1994).
- ⁴⁰M. Takigawa and D. B. Mitzi, Phys. Rev. Lett. **73**, 1287 (1994).